# Supporting Information

## Palyanov et al. 10.1073/pnas.1313340110

### SI Materials and Methods

**Starting Materials.** Starting materials consisted of natural specimens of magnesite and dolomite with an impurity content of <0.5 wt.% nd powders of chemically pure $Fe^0$ (99.999%) and presynthesized $Fe_3C$. The initial mixture of the carbonates had a bulk composition of $Mg_{0.9}Ca_{0.1}CO_3$. Weight proportions of the starting materials are shown in Table 1.

**High-Pressure Experiments.** Experiments were carried out using a multianvil high-pressure apparatus of a split-sphere type (1). High-pressure cells in the form of tetragonal prisms, 21.1 × 21.1 × 25.4 and 19 × 19 × 22 mm in size, were used at pressures of 6.5 and 7.5 GPa, respectively. The elongated geometry of the cells made it possible to use graphite heaters with a diameter of 12 mm and a length of 18.8 mm at 6.5 GPa and 9 mm in diameter and 14.8 mm long at 7.5 GPa. Pressure was calibrated by recording the change in the resistance of Bi at 2.55 GPa and of PbSe at 4.0 and 6.8 GPa at room temperature and by bracketing the graphite–diamond equilibrium at high temperatures (2). Details on the pressure and temperature calibration have been presented elsewhere (3). The temperature was measured in each experiment using a $PtRh_{30}/PtRh_6$ thermocouple. The main series of experiments was performed in the $Mg_{0.9}Ca_{0.1}CO_3$-$Fe^0$ system at pressures of 7.5 and 6.5 GPa, with temperatures in the range of 1,000–1,650 °C and 1,350–1,600 °C, respectively. The run times spanned the range from 8 to 60 h, thereby enabling examination of different stages of the reactions and the determination of both intermediate and final products. An additional series of experiments was conducted in the $Mg_{0.9}Ca_{0.1}CO_3$-$Fe_3C$ system at 7.5 GPa, in the temperature range of 1,000–1,450 °C and for a duration of 60 h. A carbonate container, made from a magnesite–dolomite mixture, was placed in the Pt capsule (6 and 10 mm in diameter at 7.5 and 6.5 GPa, respectively). A pellet of pressed iron (or cohenite) was mounted in the center of the carbonate container. This sandwich-type assembly of the reagents provided an $fO_2$ gradient over the samples and prevented the reaction between the metallic iron and Pt (Fig. S1). In relatively low-temperature experiments, cubo-octahedral synthetic diamond seed crystals ~0.5 mm in size were placed inside the carbonate containers. The assembled capsules were sealed by arc welding. The length of the sealed capsules was of 3.5–4.0 mm. The capsules were placed in the central zone of the high-pressure cells, where the temperature gradient did not exceed 10 °C/mm (3). The use of Pt capsules of relatively large volume and the sandwich-type assembly permitted a detailed study of the effects associated with the redox front propagation.

**Analytical Procedures.** After termination of the experiments, samples from different parts of the capsules were studied using X-ray and microprobe analyses, optical and scanning electron microscopy, and Raman and infrared spectroscopy. Phase identification of run products was made by X-ray diffraction (a DRON-3 diffractometer) and Raman spectroscopy. Raman spectra were measured using a Horiba J.Y. LabRAM HR800 spectrometer with an Ar-ion laser (514 nm). An investigation of phase relations and measurements of energy dispersive spectra (EDS) of various phases were performed using a Tescan MIRA3 LMU scanning electron microscope. The micromorphology of diamond crystals was studied using a Tescan MIRA3 LMU SEM and an Olympus BX51 optical microscope. Infrared absorption spectra of diamonds were measured using a Bruker Vertex 70 FTIR spectrometer fitted with a Hyperion 2000 IR microscope. Microscope apertures providing sampling areas of 50–100 μm in size were applied. To convert the recorded spectra into the absorption coefficient units, each spectrum was fitted to the standard infrared spectrum of type IIa diamond so that to obtain the best fit of the intrinsic two-phonon absorption bands (2,700–1,700 $cm^{-1}$). Nitrogen concentrations were determined by decomposing the IR spectra, in the one-phonon region (1,400–9,00 $cm^{-1}$), into A and C components, and using conversion factors of 16.5 atomic ppm·$cm^{-1}$ of absorption at 1,280 $cm^{-1}$ for the A centers (4) and 25 atomic ppm·$cm^{-1}$ of absorption at 1,130 $cm^{-1}$ for the C centers (5). Due to small sizes and irregular shape of diamonds crystallized from carbonate melt, the recorded spectra were somewhat distorted by the interference fringes. This gave rise to some uncertainty in the fitting confidence and was the major source of error in determining the absorption coefficients and, consequently, nitrogen concentrations. This error was sample dependent and, as estimated, varied within 15–20%. For diamonds crystallized in the metal-carbon melt, the error of nitrogen content calculations was ~10%. The isotopic analysis of iron carbide was performed using a Finnigan MAT-Delta isotope ratio mass spectrometer in dual inlet mode. The procedure of sample preparation was similar to that described by Deines and Wickman (6). A 20- to 25-mg sample of iron carbide was powdered and oxidized in a quartz reaction cell with pure oxygen for 60 min at 950 °C. The isotope analysis procedure was controlled with the United States Geological Survey standard USGS-24. The isotope analysis of carbonate was performed using a MAT-253 mass spectrometer in continuous flow mode using classical method of $H_3PO_4$ reaction (7). The National Bureau of Standards NBS-18 and NBS-19 standards were used to control the isotope analysis of carbonates. The reproducibility of the $\delta^{13}C$ values of both iron carbide and carbonate was 0.1‰ ($1\sigma, n = 2$). Chemical composition of mineral phases was investigated using a Cameca Camebax-Micro microprobe. For microprobe analysis, samples in the form of polished sections were prepared. Mineral phases were analyzed with a focused beam. Composition of the quenched melt was defined with a defocused beam of 20–30 μm in diameter.


1. Palyanov YN, Borzdov YM, Khokhryakov AF, Kupriyanov IN, Sokol AG (2010) Effect of nitrogen impurity on diamond crystal growth processes. *Cryst Growth Des* 10(7): 3169–3175.
2. Kennedy CS, Kennedy GC (1976) The equilibrium boundary between graphite and diamond. *J Geophys Res* 81(14):2467–2470.
3. Pal'yanov YN, Sokol AG, Borzdov YM, Khokhryakov AF (2002) Fluid-bearing alkaline-carbonate melts as the medium for the formation of diamonds in the Earth's mantle: an experimental study. *Lithos* 60(3-4):145–159.
4. Boyd SR, Kiflawi I, Woods GS (1994) The relationship between infrared absorption and the A defect concentration in diamond. *Philos Mag B* 69(6):1149–1153.
5. Kiflawi AE, et al. (1994) Infrared absorption by single nitrogen and A defect centres in diamond. *Philos Mag B* 69(6):1141–1147.
6. Deines P, Wickman FE (1975) A contribution to the stable carbon isotope geochemistry of iron meteorites. *Geochim Cosmochim Acta* 39:547–557.
7. Révész KM, Landwehr JM (2002) $\delta^{13}C$ and $\delta^{18}O$ isotopic composition of $CaCO_3$ measured by continuous flow isotope ratio mass spectrometry: Statistical evaluation and verification by application to Devils Hole core DH-11 calcite. *Rapid Commun Mass Spectrom* 16(22): 2102–2114.

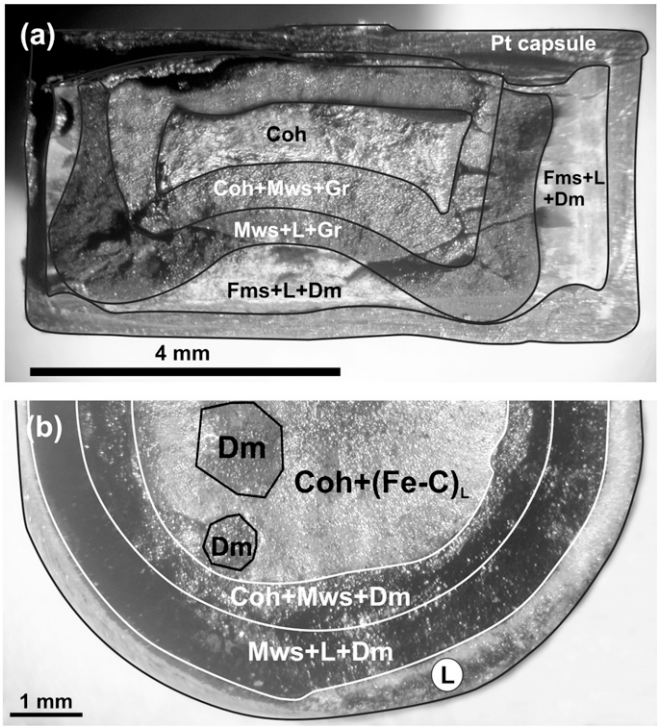


**Fig. S1.** Photomicrographs of samples from the experiments with carbonate–iron interaction: (*A*) vertical section of the sample from run N 1567 (6.5 GPa, 1,350 °C); (*B*) horizontal section of the sample from run N 1566 (6.5 GPa, 1,550 °C). Coh, cohenite ($Fe_3C$); Mws, magnesiowustite; $(Fe\text{-}C)_L$, iron-carbon melt; L, carbonate melt with dissolved magnesiowustite; Fms, ferromagnesite; Gr, graphite; Dm, diamond.

**Table S1. Representative analyses of mineral phases and melts (wt.%)**

| Run N | 1567 (6.5 GPa, 1,350 °C, 20 h) | | | | | 1250 (6.5 GPa, 1,450 °C, 20 h) | | | | | 1566 (6.5 GPa, 1,550 °C, 10 h) | | | | 1571 (6.5 GPa, 1,600 °C, 8 h) | | | | 1541 (7.5 GPa, 1,000 °C, 60 h) | | | | |
|---|---|---|---|---|---|---|---|---|---|---|---|---|---|---|---|---|---|---|---|---|---|---|---|
| Association | Coh+ Mws+Gr | Mws+ L+Gr | | Fms+ L+Dm | | Coh+ Mws+ Dm | Mws+L+ Gr+Dm | | L+Mws+ Gr+Dm | | Coh+ Mws+ Dm | Mws+L+ Gr+Dm | | L+Dm | Coh+ Mws+Dm | Mws+L+ Gr+Dm | | L+Dm | Coh+ Mws+Gr | Mws+ Marg+Gr | | Fms+Marg | |
| Phase | Mws | Mws | L | Fms | L | Mws | Mws | L | L | Mws | Mws | Mws | L | L | Mws | Mws | L | L | Mws | Mws | Marg | Fms | Marg |
| FeO | 89.2–73.5 | 70.88 | 11.0 | 1.1 | 12.1 | 82.3–79.9 | 73.6 | 10.2 | 12.0 | 72.3 | 88.9–64.7 | 54.4 | 14.3 | 16.4 | 86.9–68.2 | 52.9 | 10.3 | 15.2 | 93.5–77.1 | 74.9 | 1.4 | 2.0 | 0.8 |
| MgO | 10.3–25.8 | 28.31 | 7.2 | 43.1 | 6.0 | 16.7–19.5 | 21.3 | 5.1 | 5.4 | 25.3 | 10.9–34.6 | 42.0 | 5.8 | 19.1 | 13.0–28.3 | 46.7 | 5.1 | 17.2 | 7.0–22.6 | 25.1 | 2.2 | 46.8 | 0.9 |
| CaO | — | 0.13 | 39.2 | 6.6 | 45.6 | 0.4–0.5 | 4.4 | 44.8 | 44.7 | 2.3 | 0.2–0.8 | 3.2 | 34.3 | 15.9 | 0–3.1 | 0.1 | 44.0 | 20.3 | 0–0.1 | 0.2 | 50.8 | 2.2 | 54.8 |
| $CO_2$* | — | — | 45.8 | 49.2 | 46.9 | — | — | 39.9 | 37.9 | — | — | — | 45.6 | 48.6 | — | — | 40.6 | 47.3 | — | — | 45.6 | 49.0 | 43.4 |
| Total | 100 | 99.32 | 100.0 | 100.0 | 100.0 | 100 | 99.4 | 100.0 | 100.0 | 99.9 | 100.0 | 99.7 | 100.0 | 100.0 | 100.0 | 99.8 | 100.0 | 100.0 | 100 | 100.1 | 100.0 | 100.0 | 100.0 |
| Mg# | 0.1–0.3 | 0.36 | 0.17 | 0.93 | 0.13 | 0.2 | 0.34 | 0.12 | 0.12 | 0.39 | 0.18–0.49 | 0.56 | 0.15 | 0.48 | 0.21–0.41 | 0.61 | 0.12 | 0.43 | 0.13–0.35 | 0.38 | 0.06 | 0.95 | 0.02 |

| Run N | 1540 (7.5 GPa, 1,100 °C, 60 h) | | | | 1532 (7.5 GPa, 1,200 °C, 60 h) | | | | | 1528 (7.5 GPa, 1,300 °C, 60 h) | | | | | 1525 (7.5 GPa, 1,400 °C, 60 h) | | | | |
|---|---|---|---|---|---|---|---|---|---|---|---|---|---|---|---|---|---|---|---|
| Association | Mws+Marg+Gr | | Fms+Marg+Gr | | Mws+L+Gr | | Fms+L+Mws+Gr | | | Mws+L+Gr+ Dm | | Fms+L+Mws+Gr+Dm | | | Mws+L+Gr+ Dm | | Fms+L+Mws+Gr+Dm | | |
| Phase | Mws | Marg | Fms | Marg | Mws | L | Fms | L | Mws | Mws | L | Fms | L | Mws | Mws | L | Fms | L | Mws |
| FeO | 87.2–77.9 | 1.4 | 1.3 | 1.1 | 75.7 | 14.5 | 1.2 | 18.2 | 74.8 | 74.3 | 13.0 | 6.0 | 18.3 | 73.3 | 74.4 | 14.7 | 8.4 | 19.2 | 74.3 |
| MgO | 12.1–22.2 | 2.3 | 45.9 | 2.2 | 24.3 | 11.5 | 42.7 | 11.9 | 25.2 | 25.0 | 15.7 | 36.5 | 18.0 | 26.2 | 24.5 | 11.4 | 40.0 | 11.8 | 25.5 |
| CaO | 0–0.4 | 55.5 | 0.7 | 54.7 | — | 28.5 | 4.7 | 24.1 | — | 0.1 | 28.7 | 10.4 | 20.4 | 0.2 | 0.1 | 29.9 | 3.5 | 25.8 | 0.2 |
| $CO_2$* | — | 40.7 | 52.2 | 42.0 | — | 45.5 | 51.4 | 45.9 | — | — | 42.6 | 47.1 | 43.3 | — | — | 44.0 | 48.1 | 43.2 | — |
| Total | 100 | 100.0 | 100.0 | 100.0 | 100.0 | 100.0 | 100.0 | 100.0 | 100.1 | 99.4 | 100.0 | 100.0 | 100.0 | 99.6 | 99.0 | 100.0 | 100.0 | 100.0 | 100.0 |
| Mg# | 0.20–0.34 | 0.06 | 0.97 | 0.06 | 0.37 | 0.29 | 0.91 | 0.30 | 0.38 | 0.38 | 0.36 | 0.82 | 0.42 | 0.39 | 0.37 | 0.28 | 0.90 | 0.29 | 0.38 |

| Run N | 1517 (7.5 GPa, 1,450 °C, 30 h) | | | | | 1515 (7.5 GPa, 1,550 °C, 20 h) | | | | | 1521 (7.5 GPa, 1,650 °C, 8 h) | | | | | 1561 (7.5 GPa, 1,000 °C, 60 h) | | | | |
|---|---|---|---|---|---|---|---|---|---|---|---|---|---|---|---|---|---|---|---|---|
| Association | Mws+L+Gr+Dm | | L+Mws+Fms+Gr+Dm | | | Mws+L+Gr+ Dm | | L+Mws+Fms+Gr+Dm | | | Mws+L+Dm | | L+Mws+Fms+Dm | | | Coh+ Mws+Gr | Mws+Arg+Gr | | Fms+Arg | |
| Phase | Mws | L | L | Mws | Fms | Mws | L | L | Mws | Fms | Mws | L | L | Mws | Fms | Mws | Mws | Arg | Fms | Arg |
| FeO | 72.4 | 18.5 | 19.8 | 71.7 | 7.0 | 71.2 | 18.3 | 20.0 | 69.7 | 5.3 | 70.3 | 18.0 | 19.5 | 70.2 | 8.9 | 92.9–83.6 | 75.5 | 0.7 | 1.0 | 0.3 |
| MgO | 27.1 | 14.0 | 17.3 | 28.8 | 42.7 | 28.5 | 20.3 | 20.2 | 30.1 | 44.1 | 28.7 | 25.8 | 20.6 | 30.0 | 34.0 | 7.6–16.6 | 24.6 | 0.1 | 47.8 | 1.7 |
| CaO | — | 20.6 | 16.1 | — | 2.9 | — | 17.5 | 15.9 | 0.1 | 2.5 | 0.1 | 10.4 | 12.0 | 0.1 | 5.7 | — | 0.1 | 55.3 | 3.6 | 51.9 |
| $CO_2$* | — | 46.9 | 46.8 | — | 47.5 | — | 43.0 | 43.2 | — | 48.2 | — | 48.8 | 48.0 | — | 51.4 | — | — | 44.0 | 47.5 | 46.2 |
| Total | 100.0 | 100.0 | 100.0 | 100.6 | 100.0 | 99.7 | 100.0 | 100.0 | 99.8 | 100.0 | 99.1 | 100.0 | 100.0 | 100.3 | 100.0 | 100 | 100.2 | 100.0 | 100.0 | 100.0 |
| Mg# | 0.41 | 0.36 | 0.43 | 0.42 | 0.92 | 0.42 | 0.47 | 0.47 | 0.44 | 0.94 | 0.42 | 0.60 | 0.51 | 0.43 | 0.74 | 0.13–0.26 | 0.37 | 0.00 | 0.94 | 0.04 |

**Table S1. Cont.**

| Run N | 1560 (7.5 GPa, 1,100 °C, 60 h) | | | | | 1552 (7.5 GPa, 1,200 °C, 60 h) | | | | | | 1548 (7.5 GPa, 1,300 °C, 60 h) | | | | | | 1545 (7.5 GPa, 1,400 °C, 60 h) | | | | | |
|---|---|---|---|---|---|---|---|---|---|---|---|---|---|---|---|---|---|---|---|---|---|---|---|
| Association | Coh+ Mws+Gr | Mws+ Arg+Gr | | Fms+Arg | | Coh+ Mws+Gr | Mws+L+Gr | | Fms+L+Mws | | | Coh+ Mws+Gr | Mws+L+Gr | | Fms+L+Mws+Gr | | | Coh+ Mws+Gr | Mws+L+Gr | | Fms+L+ Mws+Gr+Dm | | |
| Phase | Mws | Mws | Arg | Fms | Arg | Mws | Mws | L | Fms | L | Mws | Mws | Mws | L | Fms | L | Mws | Mws | Mws | L | Fms | Mws | L |
| FeO | 85.9–77.8 | 71.8 | 0.8 | 0.98 | 0.1 | 84.6 | 79.8 | 12.4 | 0.8 | 12.1 | 78.1 | 75.1 | 64.3 | 15.8 | 4.7 | 17.5 | 63.5 | 68.4 | 66.1 | 17.0 | 0.8 | 63.6 | 19.4 |
| MgO | 13.6–22.1 | 27.6 | 0.0 | 43.3 | 0.1 | 13.9 | 19.9 | 15.9 | 46.7 | 14.3 | 21.9 | 24.0 | 35.0 | 13.6 | 40.0 | 13.4 | 35.4 | 31.8 | 33.7 | 12.5 | 46.4 | 35.5 | 13.0 |
| CaO | — | 0.1 | 52.9 | — | 55.0 | 0.6 | 0.1 | 20.7 | 3.5 | 23.2 | — | — | 0.1 | 24.7 | 4.2 | 25.0 | 0.2 | — | — | 26.5 | 3.8 | 0.1 | 25.6 |
| $CO_2$* | — | — | 46.3 | 55.8 | 44.9 | — | — | 51.0 | 49.1 | 50.3 | — | — | — | 45.9 | 51.1 | 44.1 | 0.00 | — | — | 44.0 | 49.0 | — | 42.0 |
| Total | 100.0 | 99.4 | 100.0 | 100.0 | 100.0 | 99.1 | 99.9 | 100.0 | 100.0 | 100.0 | 99.9 | 99.1 | 99.4 | 100.0 | 100.0 | 100.0 | 99.1 | 100.2 | 99.8 | 100.0 | 100.0 | 99.2 | 100.0 |
| Mg# | 0.22–0.34 | 0.41 | 0.00 | 0.99 | 0.01 | 0.23 | 0.31 | 0.42 | 0.94 | 0.38 | 0.33 | 0.36 | 0.49 | 0.34 | 0.88 | 0.33 | 0.50 | 0.46 | 0.48 | 0.31 | 0.94 | 0.50 | 0.31 |

Arg, aragonite; Coh, cohenite ($Fe_3C$); Dm, diamond; Fms, ferromagnesite; Gr, graphite; L, carbonate melt with dissolved magnesiowustite; Marg, Mg-aragonite; Mws, magnesiowustite.
*Calculated from a deficit of microprobe totals.